Bernardo Yusta,[1] Laurie L. Baggio,[1] Jacqueline Koehler,[1] Dianne Holland,[1] Xiemin Cao,[1] Lee J. Pinnell,[2] Kathene C. Johnson-Henry,[2] William Yeung,[2] Michael G. Surette,[3] K.W. Annie Bang,[1] Philip M. Sherman,[2] and Daniel J. Drucker[1]

GLP-1R Agonists Modulate Enteric Immune Responses Through the Intestinal Intraepithelial Lymphocyte GLP-1R

Diabetes 2015;64:2537–2549 | DOI: 10.2337/db14-1577

Obesity and diabetes are characterized by increased inflammation reflecting disordered control of innate immunity. We reveal a local intestinal intraepithelial lymphocyte (IEL)-GLP-1 receptor (GLP-1R) signaling network that controls mucosal immune responses. *Glp1r* expression was enriched in intestinal IEL preparations and copurified with markers of Tαβ and Tγδ IELs, the two main subsets of intestinal IELs. Exendin-4 increased cAMP accumulation in purified IELs and reduced the production of cytokines from activated IELs but not from splenocytes ex vivo. These actions were mimicked by forskolin, absent in IELs from *Glp1r*$^{-/-}$ mice, and attenuated by the GLP-1R agonist exendin (9-39) consistent with a GLP-1R–dependent mechanism of action. Furthermore, *Glp1r*$^{-/-}$ mice exhibited dysregulated intestinal gene expression, an abnormal representation of microbial species in feces, and enhanced sensitivity to intestinal injury following administration of dextran sodium sulfate. Bone marrow transplantation using wild-type C57BL/6 donors normalized expression of multiple genes regulating immune function and epithelial integrity in *Glp1r*$^{-/-}$ recipient mice, whereas acute exendin-4 administration robustly induced the expression of genes encoding cytokines and chemokines in normal and injured intestine. Taken together, these findings define a local enteroendocrine-IEL axis linking energy availability, host microbial responses, and mucosal integrity to the control of innate immunity.

The enteroendocrine system comprises a complex network of specialized endocrine cells situated within the epithelial lining of the stomach and small and large intestine. Gut endocrine cells synthesize and secrete dozens of peptide hormones that function as local neurotransmitters, propagating signals through engagement of the enteric nervous system. Enteroendocrine-derived hormones also act as classical hormones controlling metabolism through regulation of energy intake, digestion, absorption, and the disposal and storage of digested nutrients (1). The majority of gut hormones are secreted at low basal levels in the fasting state, and feeding produces a rapid rise in circulating levels, enabling activation of gut hormone action in response to energy intake. Plasma levels of some gut hormones, including the glucagon-like peptides, also increase rapidly in the presence of intestinal injury or mucosal inflammation (2).

Proglucagon-producing L cells are among the most intensively studied enteroendocrine cells predominantly localized to the distal small bowel and colon (3). Proglucagon liberates multiple proglucagon-derived peptides with unique biological activities, including glicentin, oxyntomodulin, and GLP-1 and GLP-2 (4). Although the actions of glicentin and oxyntomodulin remain incompletely understood, both GLP-1 and GLP-2 exert well-defined actions through distinct G-protein–coupled receptors. GLP-1 controls gut motility and food intake and stimulates insulin while simultaneously inhibiting glucagon secretion (4,5). In contrast, GLP-2 acts more locally within the gut to increase nutrient absorption and maintain the integrity of the gut epithelium (6).

[1]Department of Medicine, Mount Sinai Hospital, Lunenfeld-Tanenbaum Research Institute, Toronto, ON, Canada
[2]Cell Biology Program, Research Institute, The Hospital for Sick Children, University of Toronto, Toronto, ON, Canada
[3]Department of Medicine, Department of Biochemistry and Biomedical Sciences, Faculty of Health Sciences, McMaster University, Hamilton, ON, Canada
Corresponding author: Daniel J. Drucker, drucker@lunenfeld.ca.

Received 14 October 2014 and accepted 17 February 2015.

This article contains Supplementary Data online at http://diabetes.diabetesjournals.org/lookup/suppl/doi:10.2337/db14-1577/-/DC1.

B.Y. and L.L.B. are co-first authors.

See accompanying article, p. 2329.

Considerable evidence supports the importance of the GLP-1 system as an integral component of the incretin axis. Indeed, transient blockade of GLP-1 receptor (GLP-1R) signaling reduces insulin, increases glucagon, and impairs glucose tolerance in multiple species (4). Similarly, genetic interruption of the murine *Glp1r* impairs glucose control, establishing basal GLP-1R signaling as essential for regulation of β-cell function and glucose homeostasis. Nevertheless, the low levels of circulating active GLP-1 together with the distal location of L cells have led some to question whether the major role of GLP-1 is to function as a circulating incretin hormone (7).

More recent studies have expanded concepts of L-cell biology to encompass control of GLP-1 secretion by cytokines and bacterial products. Interleukin (IL)-6 enhances secretion of GLP-1, actions mediated by direct interaction of IL-6 with gut L cells (8). GLP-1 secretion is also induced by bacterial endotoxin, enabling lipopolysaccharide (LPS)-mediated glucoregulation through the GLP-1R (9,10). Furthermore, plasma GLP-1 levels are significantly increased in hospitalized critically ill patients (10), supporting a correlation between systemic inflammation and L-cell secretion. Nevertheless, the importance of GLP-1 in the setting of localized or systemic inflammation remains uncertain. We describe a new axis linking GLP-1R signaling to the control of immune responses in intestinal intraepithelial lymphocytes (IELs), a specialized gut immune cell population that modulates innate immunity and controls gut barrier function, epithelial turnover, and the host response to enteric pathogens (11). These findings extend our understanding of enteroendocrine-immune interactions beyond traditional glucoregulatory concepts of GLP-1 action, with implications for use of GLP-1R agonists in the treatment of metabolic disorders characterized by enhanced activity of the innate immune system.

RESEARCH DESIGN AND METHODS

Mice

Male or female C57BL/6 wild-type (WT) mice were from The Jackson Laboratory (Bar Harbor, ME) and acclimated to the animal facility for a minimum of 1 week before analysis. Whole-body $Glp1r^{-/-}$ mice on the C57BL/6 genetic background (12) and $Glp1r^{+/+}$ control mice were generated by crossing $Glp1r^{+/-}$ mice; 9–18-week-old animals from the same litter or family were studied and housed under specific pathogen-free conditions in microisolator cages and maintained on a 12-h light/dark cycle with free access to standard rodent diet and water unless otherwise noted. All experiments were carried out in accordance with protocols and guidelines approved by the Animal Care Committee at the Toronto Centre for Phenogenomics.

Isolation of Mouse Intestinal IELs, Splenocytes, and Thymocytes

Murine intestinal IELs were obtained following established protocols (13). After flushing luminal contents and removing Peyer's patches, intestines were opened longitudinally and cut in 5–10-mm pieces. Tissue fragments were incubated twice in 10 mmol/L calcium- and magnesium-free Hanks' balanced salt solution containing 1 mmol/L dithiothreitol and 5% FBS at 37°C followed by vortexing. Supernatants were combined, filtered through a 40-μm strainer, and pelleted (crude IEL preparations). IELs were further purified by centrifugation in a discontinuous 44/67% Percoll gradient. IELs were collected at the interface (Percoll-purified IEL preparations). At this stage, cells were routinely 50–75% lymphocytes, with epithelial elements accounting for the remainder. Mouse splenocytes and thymocytes were isolated by mechanical dissociation of the spleen and thymus, respectively, followed by red blood cell lysis.

cAMP Analysis

Sorted IELs, splenocytes, or thymocytes were allowed to recover for 1 h and then challenged for 15 min at 37°C with exendin-4 (Ex-4) (CHI Scientific, Maynard, MA), prostaglandin E_2 (5 μmol/L; Sigma-Aldrich Canada), or the adenylyl cyclase activator forskolin (Fk) in Hanks' balanced salt solution buffer containing 0.1% BSA and 300 μmol/L 3-isobutyl-1-methylxanthine. cAMP concentration was measured using a LANCE cAMP Detection Kit (PerkinElmer, Waltham, MA) and an EnVision Multilabel Plate Reader (PerkinElmer).

Activation Assays in IELs and Splenocytes

Freshly isolated splenocytes and sorted untouched IELs were stimulated in vitro with plate-bound anti-CD3 (clone 145-2C11) and soluble anti-CD28 (clone 37.51) monoclonal antibodies (mAbs) in culture medium (RPMI + 10% FBS + 50 μmol/L β-mercaptoethanol) in the presence or absence of Ex-4, exendin (9-39) (Bachem, Torrance, CA), or Fk. After incubation for 5 h at 37°C, cells were harvested for quantitative RNA and cAMP analyses.

Dextran Sodium Sulfate–Induced Colitis

$Glp1r^{+/+}$ or $Glp1r^{-/-}$ female mice were maintained on drinking water containing 3% (weight for volume) dextran sodium sulfate (DSS) (molecular weight 40,000–50,000; USB, Cleveland, OH) or regular drinking water ad libitum for 7 days. Water intake and body weights were determined daily. Animals were euthanized on day 8, and for each mouse, a disease activity index score was calculated (14). Colon damage scores were determined as described (15). In acute studies, C57BL/6 male mice were maintained on drinking water containing 3% (weight for volume) DSS ad libitum for 4 days. On the fourth day, mice were switched to regular drinking water and given two subcutaneous injections of 10 nmol/kg Ex-4 or PBS separated by 12 h. Mice were killed the following morning for analysis of the small bowel and colon.

Histology and Immunohistochemistry

Intestinal tissue segments were fixed in 10% neutral buffered formalin and paraffin embedded. Digital image

acquisition and morphometry were performed on 5-μm histological sections stained with hematoxylin-eosin as described (16). To quantify IELs, sections were stained with a rabbit polyclonal anti-CD3 antibody (Dako Canada, Burlington, ON, Canada) and counterstained with hematoxylin. A minimum of 20 villi/section from three to four sections per tissue sample were scored.

Generation of Bone Marrow Chimeras

Bone marrow chimeras were generated by lethally irradiating *Glp1r*$^{+/+}$ or *Glp1r*$^{-/-}$ female mice (1,100 cGy split into two equal doses 4 h apart) followed by reconstitution with 5×10^6 bone marrow cells from donor C57BL/6 male mice as described (17). Mice were euthanized 12–14 weeks after bone marrow transplantation. Chimerism was assessed by quantitative PCR (qPCR) analysis for the sex-determinant Y chromosome (*Sry*) using spleen DNA from recipient mice. The efficiency of reconstitution of WT *Glp1r* expression within the intestinal compartment of recipient mice was assessed by qPCR.

RNA Isolation and Analysis of mRNA Expression

Total RNA was extracted using guanidinium isothiocyanate (18). cDNA synthesis and assessment of full-length *Glp1r* mRNA expression were performed as described (16,19). Real-time qPCR was performed on an ABI PRISM 7900HT Sequence Detection System (Applied Biosystems, Foster City, CA) with TaqMan Universal PCR Master Mix and TaqMan Gene Expression Assays (Applied Biosystems). Quantification of transcript levels was performed by the $2^{-\Delta Ct}$ method using 18S rRNA, cyclophilin, *Tbp*, or β-actin for normalization.

Gut Microbiota Analysis

Fecal DNA extraction and 16S rRNA gene amplification were carried out as previously described (20). Microbial population similarities within and between groups of *Glp1r*$^{+/+}$ and *Glp1r*$^{-/-}$ mice were determined using metagenomic analysis as described (21). A cluster analysis tree was generated using UPGMA (unweighted pair group method with arithmetic mean) cluster analysis of Bray-Curtis dissimilarity coefficients.

Statistical Analysis

Except where indicated, data are presented as mean ± SD or SE. Statistical significance was determined by unpaired two-tailed Student *t* test or one- or two-way ANOVA with Bonferroni post hoc analysis using GraphPad Prism version 5.02 software (San Diego, CA). $P < 0.05$ was considered statistically significant.

RESULTS

The *Glp1r* Is Expressed in Murine Intestinal IELs

Recent studies highlighted limitations of commercially available antisera for detection of immunoreactive GLP-1R expression (16,22). To localize cellular sites of intestinal *Glp1r* expression beyond the enteric nervous system (23), we fractionated the murine small intestine by sequential collagenase digestion followed by analysis of *Glp1r* expression and simultaneous assessment of cell lineage–specific RNA transcripts. Quantitatively, *Glp1r* expression segregated with markers of the villus epithelial compartment (Supplementary Fig. 1*A*, fraction 1) rather than the crypt compartment, mesenchyme, or smooth muscle layer (Supplementary Fig. 1*A*, fraction 2). Unexpectedly, a marked increase in relative *Glp1r* expression was observed in RNA obtained from intestinal cell preparations enriched in IELs (Fig. 1*A* and *B*). Consistent with IEL *Glp1r* expression, we detected abundant expression of IEL markers such as integrin α E (*Itgae*) and the T-cell surface glycoprotein CD3 γ (*CD3g*) in RNA from purified small bowel IELs (Fig. 1*A*). Moreover, the level of *Glp1r* expression in the intestinal IEL compartment was considerably higher than in other mouse primary and secondary lymphoid organs (Fig. 1*B*). A 1.4-kb product corresponding to the entire coding region of the canonical mouse *Glp1r* was amplified from RNA obtained from Percoll-purified IELs at levels approximating those detected in RNA from mouse lung (24) (Fig. 1*C*). Cloning and sequencing of the 1.4-kb IEL *Glp1r* mRNA transcript demonstrated that it corresponded to the sequence of the canonical murine *Glp1r* (data not shown).

Because Tαβ and Tγδ IELs represent the two major subsets of intestinal IELs, we assessed *Glp1r* expression in RNA from Percoll-purified and FACS-sorted IEL subsets isolated from the small intestine, revealing abundant *Glp1r* expression in both IEL subsets (Fig. 1*D*). Furthermore, we detected a strong correlation between levels of *Glp1r* mRNA and the relative abundance of transcripts corresponding to the IEL markers *Itgae* and *CD3g* along the entire murine small intestine and colon (Supplementary Fig. 1*B*). Taken together, these findings identify the IEL as a previously unrecognized site of *Glp1r* expression in the small and large bowel.

Neither Loss of GLP-1R Signaling nor Chronic GLP-1R Agonist Treatment of WT Mice Alters Intestinal IEL Number or Subset Composition

To determine whether the presence or absence of GLP-1R signaling alters IEL homeostasis, we compared the frequency of IELs in the small intestine and colon of *Glp1r*$^{-/-}$ versus *Glp1r*$^{+/+}$ mice and in C57BL/6 mice treated with liraglutide or saline for 1 week (Fig. 2). No significant differences in the phenotypic composition of the IEL population were detected in the small intestine or colon of *Glp1r*$^{-/-}$ versus *Glp1r*$^{+/+}$ littermate control mice (Fig. 2*A*). Furthermore, loss of GLP-1R signaling did not affect IEL density in the jejunum (Fig. 2*B*). Likewise, liraglutide had no impact on IEL density in the small intestine (Fig. 2*C*). Thus, GLP-1R signaling is not critical for IEL development or recruitment to the intestinal niche.

Activation of the GLP-1R on Murine Intestinal IELs Suppresses Expression of Inflammatory Cytokines

To assess whether the IEL *Glp1r* mRNA transcript encodes a functional GLP-1R protein, we measured levels of

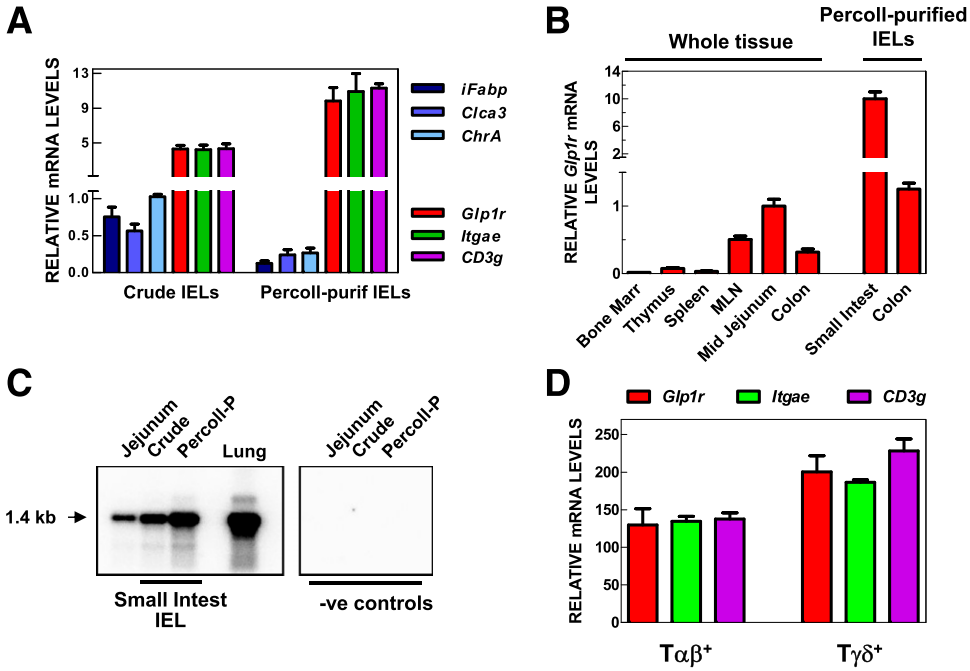

Figure 1—A canonical *Glp1r* transcript is expressed in murine intestinal IELs. *A*: *Glp1r* expression copurifies with markers of IELs from mouse small intestine. IELs were isolated from the small intestine and analyzed before (crude IELs) and after enrichment by centrifugation through a discontinuous Percoll gradient (Percoll-purified IELs). mRNA levels are expressed relative to the corresponding jejunal transcript levels and are mean ± SD of three independent IEL preparations. *iFabp*, intestinal fatty acid binding protein; *Clca3*, chloride channel calcium activated 3; *ChrA*, chromogranin A. *B*: The *Glp1r* is widely expressed in mouse lymphoid organs but at levels much lower than in intestinal IEL preparations. *Glp1r* mRNA levels are expressed relative to the *Glp1r* mRNA content in midjejunum and are mean ± SD. n = 3–6 mice for bone marrow (Bone Marr), thymus, spleen, and mesenteric lymph node (MLN); n = 11 mice for jejunum and colon; n = 6 and 3 independent preparations for small intestine and colon IELs, respectively. *C*: The mouse *Glp1r* transcript was identified in RNA isolated from the indicated sources following reverse transcription PCR with primers that amplify a 1.4-kb product encompassing the majority of the *Glp1r* open reading frame. Southern blotting with an internal *Glp1r* ^{32}P-labeled oligonucleotide was used to detect the *Glp1r* PCR product. Lung was used as a positive control for *Glp1r* expression. Negative controls (-ve controls) correspond to PCR reactions performed in the absence of first-strand cDNA synthesis. Percoll-P, Percoll purified. *D*: The *Glp1r* is expressed in both Tαβ and Tγδ IELs from mouse small intestine. Percoll-purified IELs were stained with fluorescently labeled mAbs, and Tαβ and Tδγ were purified by FACS. mRNA levels are expressed relative to jejunal mRNA levels and are mean ± SD from three independent cell-sorting experiments, each involving pooled IELs obtained from five to six mice.

cAMP in sorted nonactivated IELs in response to Ex-4 (Fig. 3*A* and *B*). Ex-4 directly increased cAMP levels in a dose-dependent manner (half-maximal effective concentration 0.35 nmol/L). Furthermore, the relative extent of Ex-4–induced cAMP production was preserved in activated IELs and was comparable in magnitude to the cAMP response triggered by 10 μmol/L Fk (Fig. 3*B*). Surprisingly, IELs exhibited a modest cAMP response to the adenylyl cyclase activator Fk compared with T cells from the thymus (Supplementary Fig. 1*C*). Because IELs produce a broad spectrum of cytokines that play key roles in intestinal inflammation, pathogen clearance, and epithelial barrier function (25), we examined whether GLP-1R signaling modified cytokine expression in sorted intestinal IELs in vitro. As a control, we examined splenocytes that express low levels of *Glp1r* mRNA. Following activation by immobilized anti-CD3 and soluble anti-CD28 antibodies, transcript levels of the proinflammatory cytokines IL-2, IL-17a, interferon γ, and tumor necrosis factor-α robustly increased in isolated IELs and splenocytes (Fig. 3*C*). Ex-4 significantly attenuated the induction of both mRNA expression and protein production of proinflammatory cytokines in IELs but not in splenocytes (Fig. 3*C* and Supplementary Fig. 1*E*). Notably, the magnitude of reduction in cytokine expression in IELs after Ex-4 treatment paralleled reductions observed with Fk (Fig. 3*C*). The actions of Ex-4 to suppress cytokine induction required the canonical GLP-1R because they were not detected in IELs from *Glp1r*$^{-/-}$ mice (Fig. 3*D*). Moreover, the GLP-1R antagonist exendin (9-39) attenuated the Ex-4–dependent suppression of cytokine mRNA expression (Supplementary Fig. 1*D*). In contrast, Fk robustly inhibited cytokine upregulation in IELs from *Glp1r*$^{-/-}$ mice (Fig. 3*D*). These findings link direct activation of GLP-1R signaling to attenuation of proinflammatory cytokine expression in IELs.

The Severity of Intestinal Injury Is Increased in *Glp1r*$^{-/-}$ Mice

IELs play an important role in maintaining the integrity of the epithelial barrier (15). Baseline small intestinal permeability assessed following ^{14}C-mannitol oral gavage was not different in *Glp1r*$^{+/+}$ versus *Glp1r*$^{-/-}$ mice (Supplementary

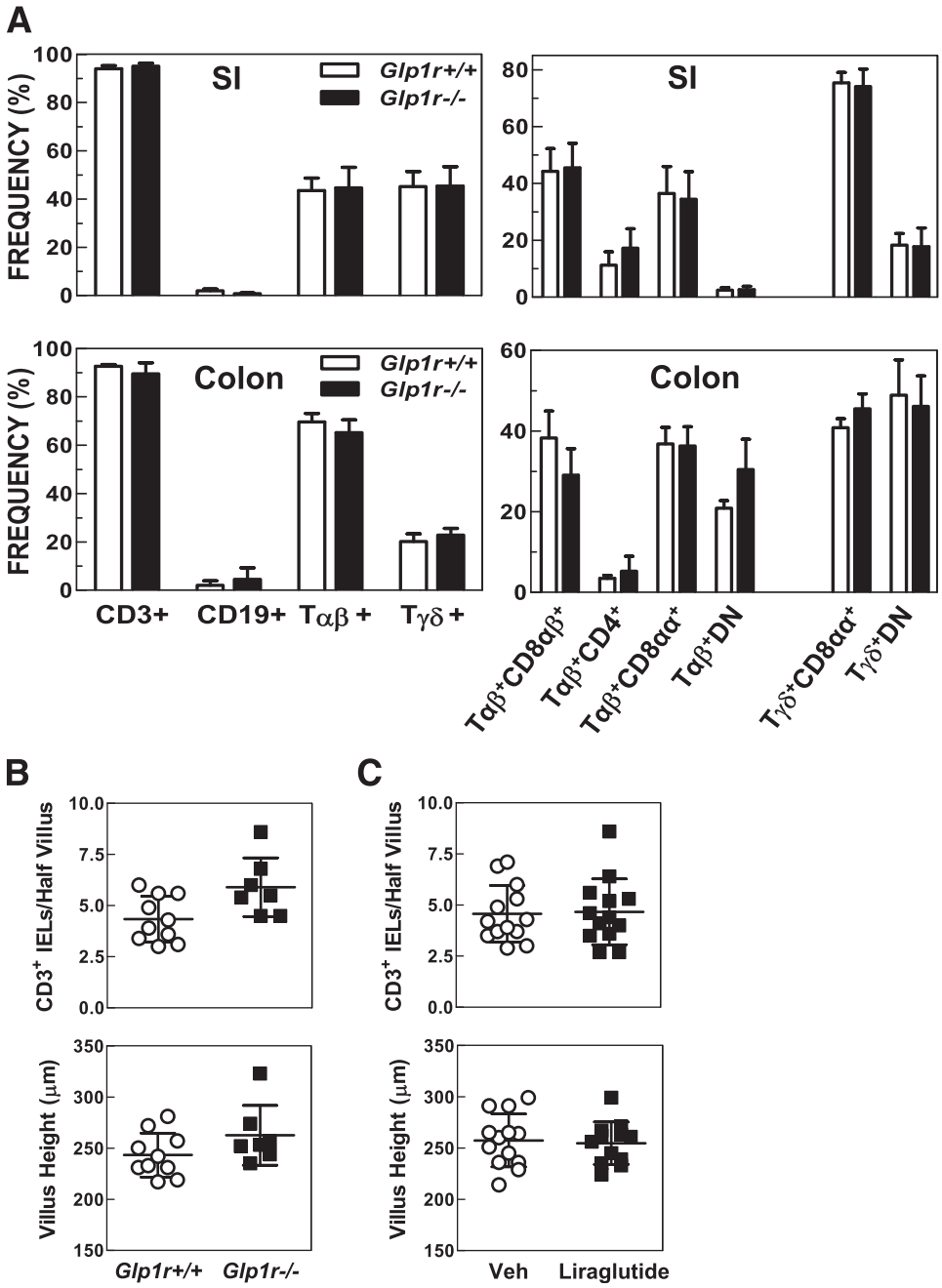

Figure 2—Loss of GLP-1R signaling does not alter the phenotypic composition of the mouse intestinal IEL population. *A*: IELs isolated from small intestine (SI) and colon were stained with fluorescently labeled mAbs and analyzed by flow cytometry. Left panels indicate the frequency expressed relative to $CD45^+$ live events within the lymphocyte gate. Right panels are frequencies of the various subpopulations of Tαβ and Tγδ IELs expressed relative to the total number of Tαβ and Tγδ cells, respectively. Data are mean ± SD (small intestine: $n = 6$ $Glp1r^{+/+}$ and 9 $Glp1r^{-/-}$ mice; colon: $n = 3$ mice of each genotype). DN, $CD4^-CD8^-$ double-negative T cells. *B* and *C*: Neither loss of GLP-1R signaling nor chronic treatment with liraglutide affected IEL density in the mouse jejunum. Jejunal IEL number (top panels) and villus height (bottom panels) in $Glp1r^{-/-}$ and $Glp1r^{+/+}$ mice (*B*) and in C57BL/6 mice following administration of the GLP-1R agonist liraglutide (75 μg/kg) or PBS vehicle (Veh) twice a day for 7 days (*C*). Jejunum tissue sections were stained with anti-CD3 antibody and the number of IELs per half-villus and the villus length scored in a blinded manner. Each data point corresponds to one mouse. $n = 7$–13 mice/group. Data in *C* are combined from two independent experiments.

Fig. 3*A*). To evaluate the importance of *Glp1r* in the setting of mucosal injury, we compared the severity of DSS-induced colitis in $Glp1r^{-/-}$ versus $Glp1r^{+/+}$ mice. $Glp1r^{-/-}$ mice lost significantly more weight despite similar intake of DSS (Fig. 4*A* and *B*); colon lengths were shorter at baseline yet reduced to a comparable extent after DSS (Fig. 4*C*). Furthermore, $Glp1r^{-/-}$ mice exhibited significantly increased disease activity scores (Fig. 4*D*) and greater epithelial damage (Fig. 4*E*) reflected by a greater colon damage score (Fig. 4*F*).

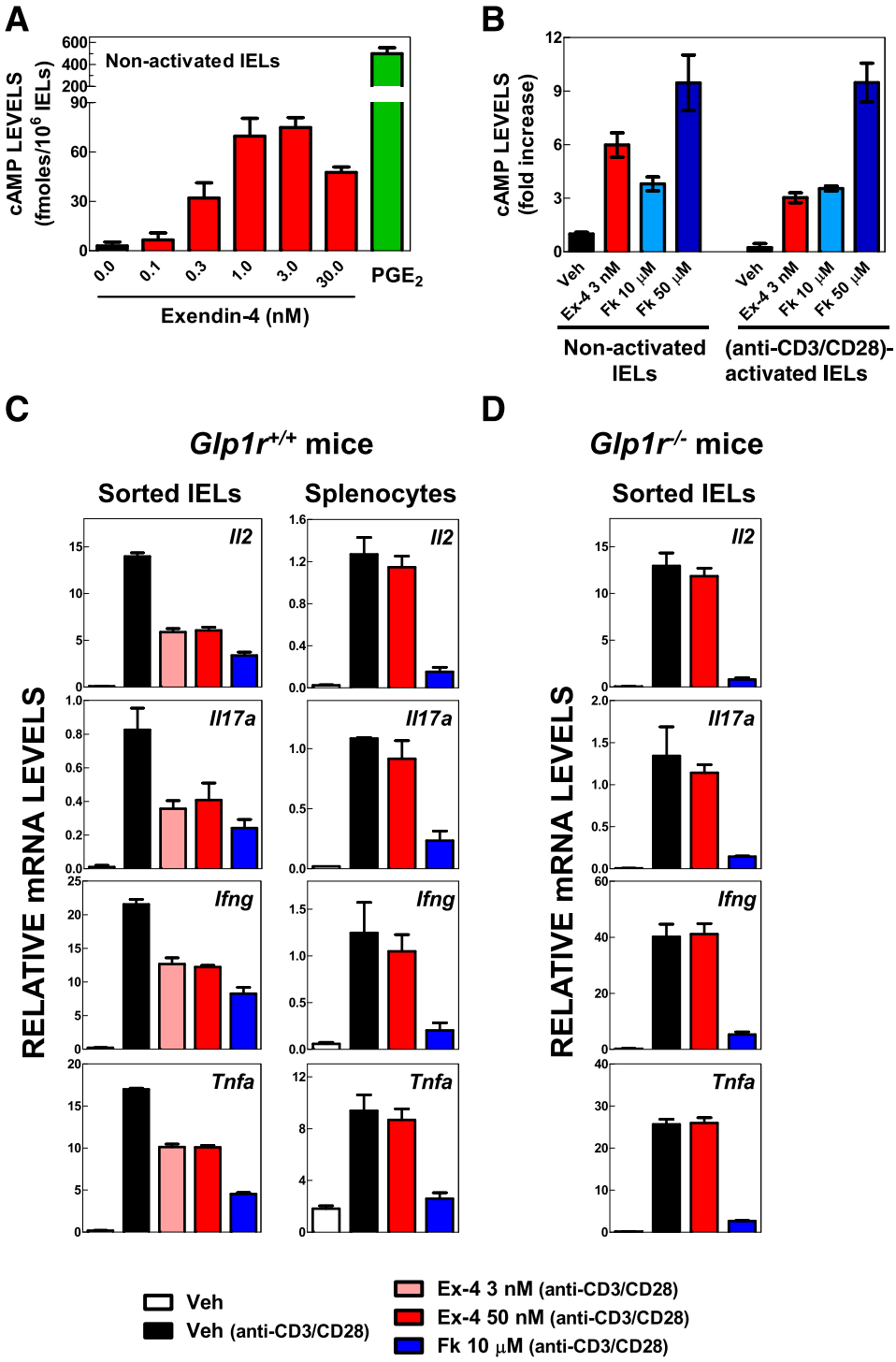

Figure 3— Murine intestinal IELs express a functional GLP-1R. *A*: Ex-4 stimulates cAMP accumulation in nonactivated IELs from *Glp1r*$^{+/+}$ mouse small intestine. Levels of cAMP were quantified in sorted untouched IELs following incubation with increasing concentrations of Ex-4. Prostaglandin E_2 (PGE_2) (5 μmol/L) was used as a positive control. Shown are combined data (mean ± SD) of two independent batches of sorted cells assayed in triplicate. *B*: Ex-4 and Fk 10 μmol/L induce comparable increases in cAMP in both activated and nonactivated IELs. Sorted untouched IELs were incubated for 5 h without (nonactivated IELs) or with (activated IELs) anti-CD3/CD28 antibodies. The cells were then challenged with Ex-4, Fk, or vehicle alone (Veh) for 15 min, and cAMP content was quantified. Data are relative to the cAMP levels in Veh-treated nonactivated IELs and are mean ± SD of four independent experiments with two or three replicates each. *C* and *D*: Ex-4 suppresses the induction of cytokine expression in activated IELs from *Glp1r*$^{+/+}$ (*C*) but not *Glp1r*$^{-/-}$ (*D*) mouse small intestine. Splenocytes and sorted untouched IELs were activated with anti-CD3/CD28 for 5 h in the presence of Ex-4, Fk, or Veh. mRNA levels of the indicated cytokines were assessed by qPCR. Data in *C* are mean ± SD of one out of five independent experiments with similar results assayed in duplicate or triplicate. Data in *D* are from a single experiment assayed in triplicate.

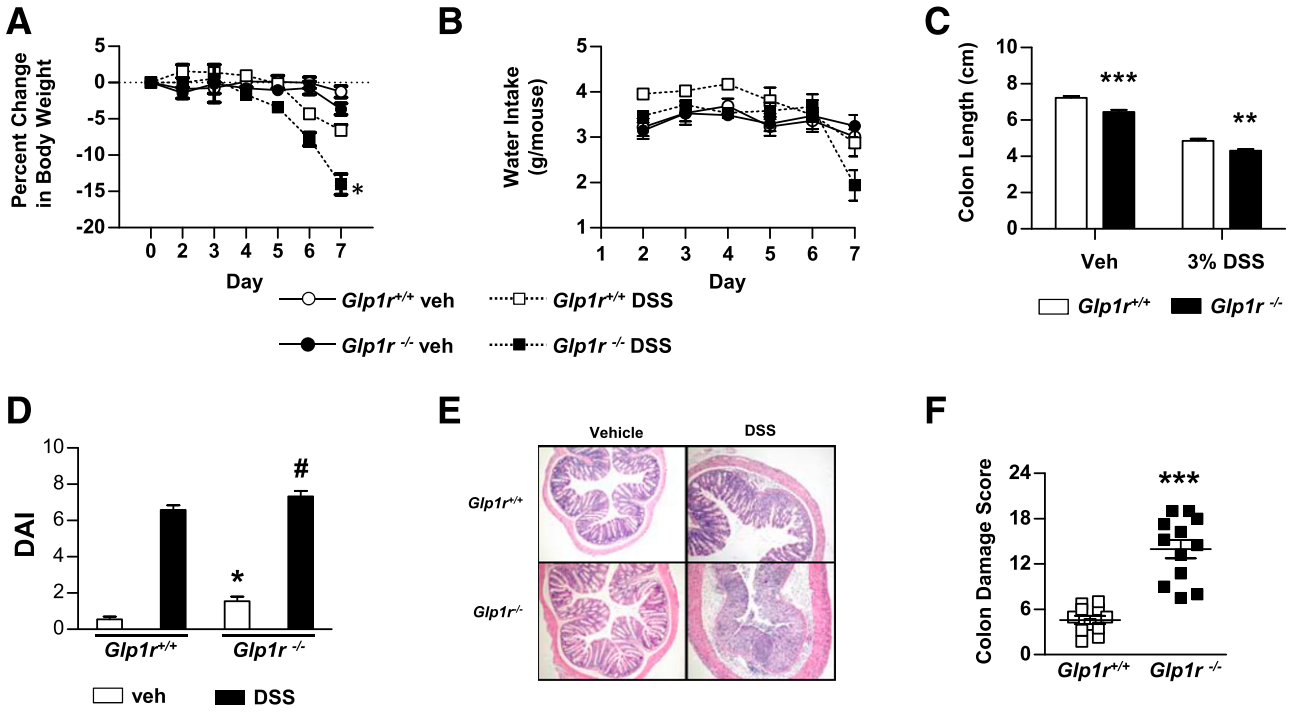

Figure 4—The severity of DSS-induced colitis is increased in *Glp1r*$^{-/-}$ mice. *Glp1r*$^{+/+}$ or *Glp1r*$^{-/-}$ mice were maintained on either regular drinking water (Veh) or water supplemented with 3% DSS for 7 days. Body weight and water intake were measured daily for the duration of the treatment. Change in body weight (*A*), daily water intake (*B*), colon length (*C*), disease activity index (DAI) (*D*), colon histology (*E*), and colon damage score (*F*) were recorded. For *A–F*, n = 9–12 mice/group. *$P < 0.05$, **$P < 0.01$, ***$P < 0.001$ vs. *Glp1r*$^{+/+}$ (*A*, *C*, and *F*). *$P <$ 0.05 vs. *Glp1r*$^{+/+}$ Veh; #$P < 0.05$ vs. *Glp1r*$^{+/+}$ DSS (*D*).

Intestinal GLP-1R Signaling Modulates the Expression of Genes Involved in Immune Regulation and Epithelial Protection and Repair

To understand how GLP-1R signaling controls mucosal integrity, we examined expression of genes important for epithelial repair, barrier function, and immune regulation in the colon of *Glp1r*$^{-/-}$ and *Glp1r*$^{+/+}$ mice in the presence or absence of DSS-induced colitis (Fig. 5 and Supplementary Fig. 2). Remarkably, even in the absence of experimental gut injury, *Glp1r*$^{-/-}$ mice exhibited significant reductions in expression of genes that contribute to epithelial protection and repair (trefoil factor [*Tff*]-1 and -2, transforming growth factor [*Tgf*]-b1 and -3, epidermal growth factor receptor [*Egfr*], keratinocyte growth factor [*Fgf7*], hepatocyte growth factor [*Hgf*]), the innate immune response (*Il6*, *Il1b*), and inflammation (*Il12b*). Furthermore, induction of gut injury with DSS produced differential colonic gene expression (*Tff3*, *Tgfb2*, *Ifng*, *Hgf*) in *Glp1r*$^{+/+}$ versus *Glp1r*$^{-/-}$ mice. These findings illustrate that GLP-1R signaling regulates genes important for intestinal homeostasis in the presence and absence of gut inflammation.

Bone Marrow Radiation Chimeras Establish the Essential Role of the IEL GLP-1R for Control of Intestinal Gene Expression

Because dysregulated intestinal gene expression in *Glp1r*$^{-/-}$ mice potentially reflects loss of GLP-1R signaling in intestinal and extraintestinal cell types, we reassessed colonic gene expression after transplantation of bone marrow from C57BL/6 male donor mice into *Glp1r*$^{-/-}$ or *Glp1r*$^{+/+}$ recipient females. In such a setting, *Glp1r*$^{-/-}$ mice are reconstituted with *Glp1r*$^{+/+}$ hematopoietic stem cells, including IELs. Chimerism, assessed in spleen DNA from the recipient mice by qPCR, was 84.3 ± 6.4%. Analysis of *Glp1r* expression in jejunum and sorted IELs from *Glp1r*$^{-/-}$ and *Glp1r*$^{+/+}$ recipient females demonstrated that IELs derived from transplanted marrow repopulated the intestinal compartment (Supplementary Fig. 3*B*). The reconstitution efficiency of *Glp1r* expression in the jejunum and IELs of *Glp1r*$^{-/-}$ recipients 12 weeks after bone marrow transplantation was 64% and 73%, respectively. We focused our analysis on genes shown in Fig. 5 to be dysregulated in the colon of *Glp1r*$^{-/-}$ mice. Selective re-establishment of WT IELs in the intestinal mucosa of *Glp1r*$^{-/-}$ mice normalized gene expression profiles for the majority of genes examined (Fig. 6).

Acute Ex-4 Administration Attenuates Edema and Increases Expression of Immunomodulatory and Antimicrobial Genes in the Small Intestine

IELs control intestinal barrier function and repair and protect the intestinal mucosal epithelium by promoting pathogen clearance and lysing pathogen-infected cells (26). Accordingly, we examined expression of immunomodulatory genes in the jejunum of C57BL/6 mice in response to Ex-4 administration (Fig. 7*A*). Ex-4 markedly upregulated levels of *Il1b*, *Il6*, *Il22*, *Il12b*, *Tnfa*, *Ccl2*, *Cxcl1*,

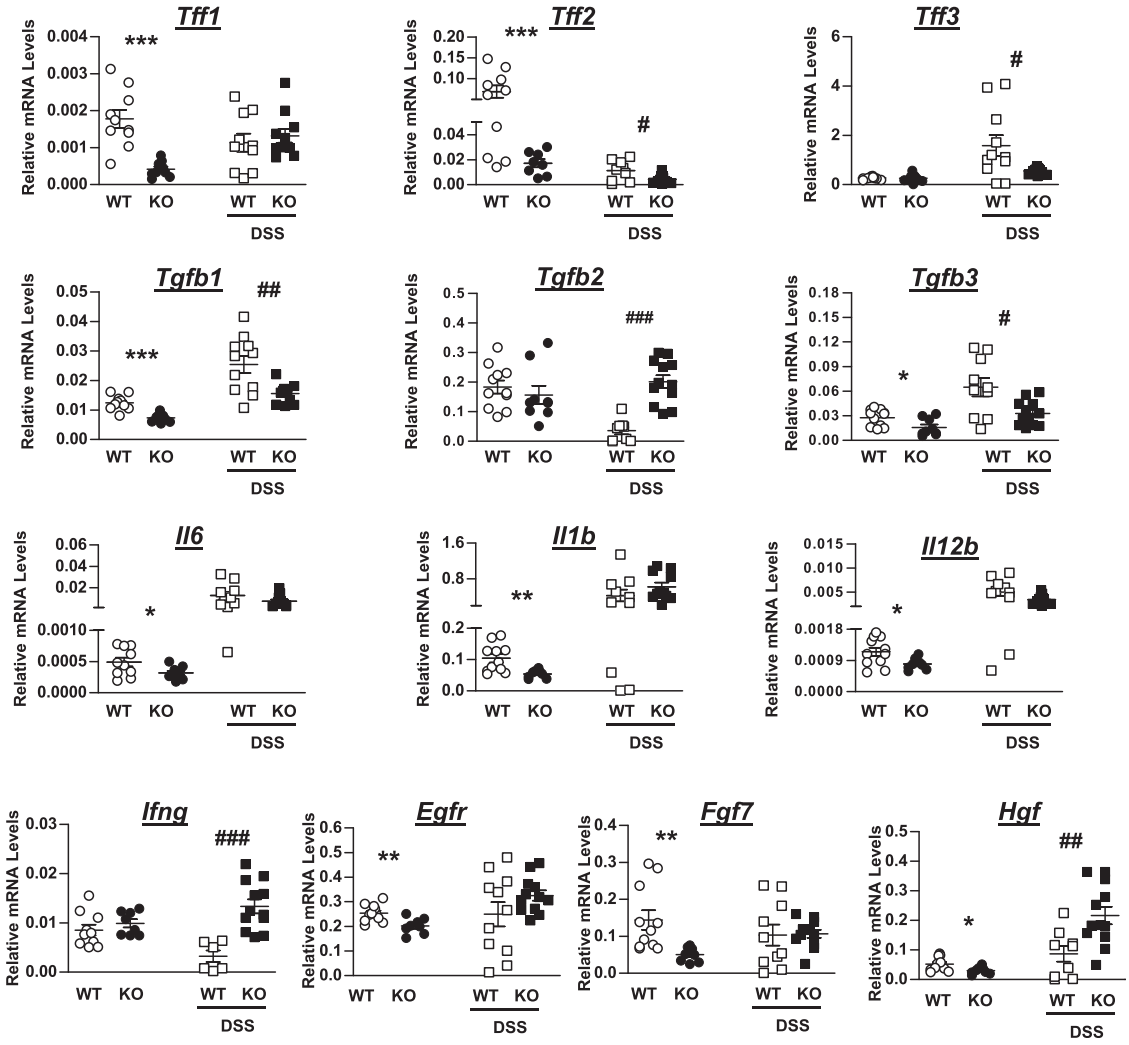

Figure 5—GLP-1R signaling modulates the colonic expression of genes important for immune regulation and epithelial protection and repair. Gene expression was examined in colonic RNA samples from *Glp1r*$^{+/+}$ (WT) or *Glp1r*$^{-/-}$ (knockout [KO]) mice (n = 8–12 mice/group) maintained on regular drinking water or drinking water supplemented with 3% DSS for 7 days. *P < 0.05, **P < 0.01, ***P < 0.001 for *Glp1r*$^{+/+}$ vs. *Glp1r*$^{-/-}$ on regular drinking water; #P < 0.05, ##P < 0.01, ###P < 0.001 for *Glp1r*$^{+/+}$ vs. *Glp1r*$^{-/-}$ on DSS drinking water.

and *Cxcl2* mRNA transcripts. The augmentation of gene expression by Ex-4 was rapid, detectable by 4 h, and transient, with levels of most mRNA transcripts returning to normal by 24 h. Increases in IL-6 and tumor necrosis factor-α protein levels were also observed 4 h after Ex-4 administration (Supplementary Fig. 3*C*). Ex-4 also significantly increased expression of genes that *1*) encode antimicrobial proteins (regenerating islet-derived protein 3 [RegIII]γ and RegIIIβ) or *2*) play a role in pathogen clearance (IL-5, IL-13). For some genes, the Ex-4–dependent induction of this group of genes, particularly *RegIIIg* and *RegIIIb*, was sustained with continued Ex-4 treatment (Fig. 7*A*). These data suggest that activation of GLP-1R signaling establishes a generalized cytoprotective response in the murine intestine.

Assessing the effects of Ex-4 or liraglutide in mice with DSS-induced colitis was complicated by marked GLP-1R agonist–mediated reductions in water and, hence, DSS intake, which attenuated intestinal injury. Consequently, we first induced intestinal injury with DSS for 4 days and then treated mice with two injections of Ex-4 12 h apart. Acute Ex-4 had no effect on body weight, colon length, or colon damage score (Fig. 7*B* and Supplementary Fig. 3*D*) but significantly reduced colon weight (Fig. 7*B*) consistent with a reduction of DSS-induced colitis-associated edema. Ex-4 significantly upregulated expression of inflammatory, antimicrobial, and growth factor genes in the ileum (Fig. 7*C*). Because IELs play important roles in host mucosal defense and response to microbial pathogens, we examined the population of major microbial species by analysis of 16S bacterial rRNA genes in the feces of *Glp1r*$^{-/-}$ versus *Glp1r*$^{+/+}$ mice (Fig. 8*A*). Remarkably, highly significant differences in the relative abundance of *Gammaproteobacteria*, *Bacteroidetes*, *Firmicutes*, and *Actinobacteria* were detected. *Bacteroidetes* and *Firmicutes* represented the majority of the bacterial population in both *Glp1r*$^{-/-}$ and *Glp1r*$^{+/+}$ mice

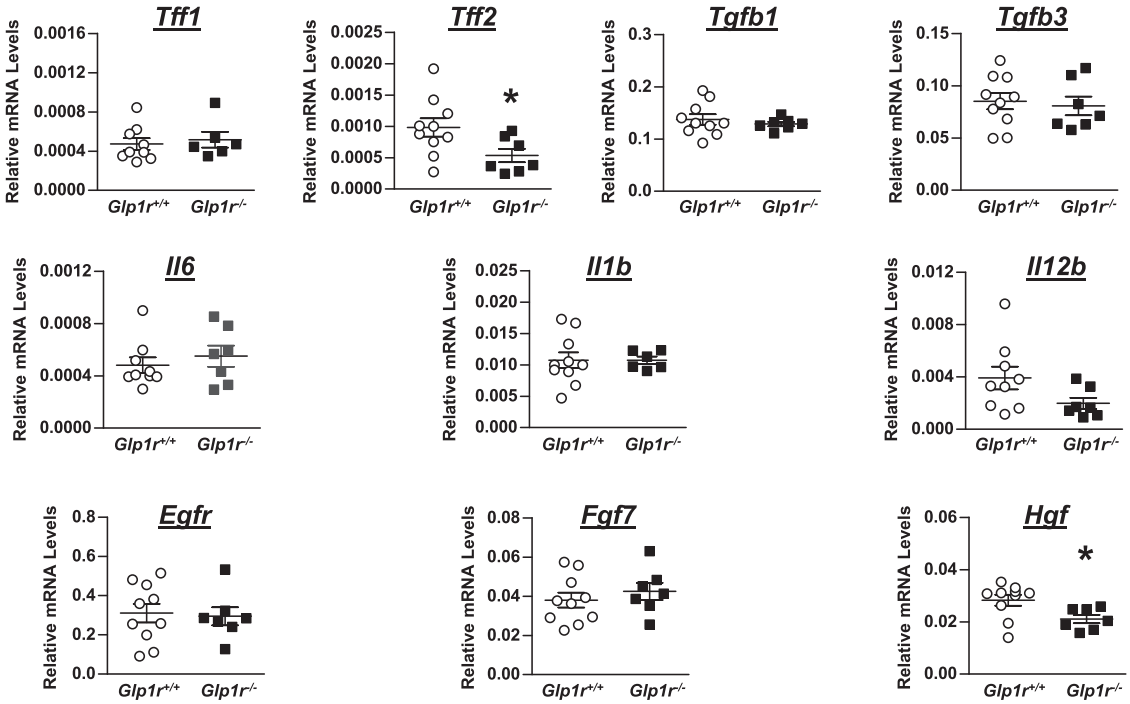

Figure 6—Normalization of colonic gene expression in *Glp1r*$^{-/-}$ mice after bone marrow transplantation. Following whole-body irradiation and bone marrow transplantation from C57BL/6 donor male mice, gene expression was examined in colonic RNA samples from recipient *Glp1r*$^{+/+}$ or *Glp1r*$^{-/-}$ female mice (n = 4–10 mice/group). *$P < 0.05$ vs. *Glp1r*$^{+/+}$.

(Supplementary Fig. 4*A*). Less similarity of microbial profiles was seen between groups than within groups. Taken together, these findings suggest that GLP-1R signaling influences the establishment of the gut microbiome and the normal host immune response to intestinal injury.

DISCUSSION

GLP-1R is expressed in the small intestine and colon (23,27); however, previous efforts to identify cellular sites of GLP-1R expression within the gut yielded conflicting results. Using a GLP-1R antibody and immunohistochemistry, Kedees et al. (28) reported GLP-1R expression in the intestinal mucosa, enteric nervous system, and Paneth cells, whereas studies using the GLP-1R promoter to direct expression of a fluorescent reporter protein localized intestinal GLP-1R expression to enteric neurons (23). GLP-1Rs have also been localized to gastric parietal cells in rats (29) and in the Brunner's gland of the duodenum, parietal cells and smooth muscle cells in the gastric muscularis externa, and myenteric plexus neurons throughout the primate small and large bowel (30). Given the lack of specificity of the majority of commercially available GLP-1R antibodies and existing discrepancies in studies reporting sites of intestinal GLP-1R expression, we initiated studies to localize the sites of endogenous GLP-1R mRNA expression in the murine gut.

Although mRNA transcripts encoding a functional GLP-1R were detected in rodent immune cells isolated from spleen, lymph nodes, and bone marrow (19), the current experiments reveal that IEL *Glp1r* expression is considerably more abundant relative to *Glp1r* mRNA levels in other mouse lymphoid organs. Several lines of evidence support the functional importance of the newly described IEL GLP-1R. First, Ex-4 directly increased cAMP accumulation in isolated IELs. Second, Ex-4 robustly suppressed expression of cytokines following activation of IELs from WT mice but had no effect on IELs from *Glp1r*$^{-/-}$ mice. Furthermore, reconstitution of *Glp1r*$^{-/-}$ mice with bone marrow from C57BL/6 donors normalized the expression of immune-related genes in the intestine. Taken together, these findings establish the functional importance of the intestinal IEL GLP-1R.

The delineation of an enteroendocrine-immune axis is not without precedent. Infection of severe combined immunodeficient mice with *Trichuris muris* reduced the number of enteroendocrine cells compared with WT controls, whereas the number of gut endocrine cells increased significantly following reconstitution of immunodeficient mice with CD4$^+$ T cells from infected WT mice (31). Furthermore, bacterial-derived products such as LPS and flagellin independently modulated expression of genes encoding peptide hormones and multiple ligands and receptors important for the immune response in LCC-18 enteroendocrine cells (32). Conversely, receptors for vasoactive intestinal peptide and pituitary adenylate cyclase–activating peptide have been localized to intestinal IELs (33), whereas Toll-like receptors are expressed on enteroendocrine cells, and Toll-like receptor activation by bacterial products promotes secretion of cholecystokinin from gut endocrine cells (34).

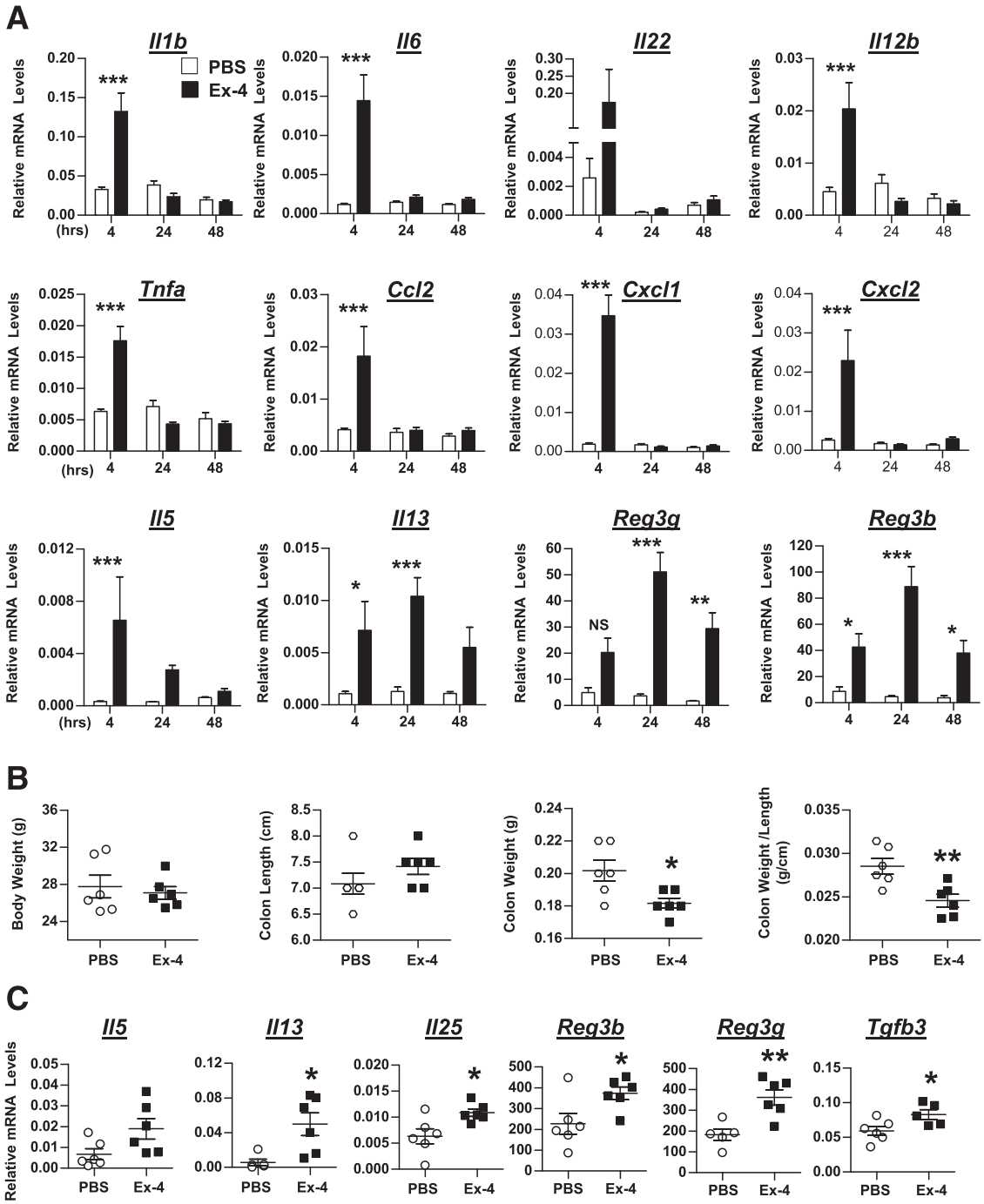

Figure 7—Acute GLP-1R agonist treatment increases the expression of immunomodulatory and antimicrobial genes in the murine small intestine. *A*: C57BL/6 mice were treated with Ex-4 (10 nmol/kg) or PBS every 12 h for up to 48 h. Mice were euthanized at 4, 24, and 48 h after the last injection. $n = 5$ mice/group. *$P < 0.05$, **$P < 0.01$, ***$P < 0.001$ vs. PBS at the same time point. NS, not significant. *B*: Body weight, colon length, colon weight, and colon weight per unit length. *C*: Ileal levels of selected mRNA in C57BL/6 mice maintained on drinking water supplemented with 3% DSS for 4 days followed by two injections (12 h apart) of Ex-4 (10 nmol/kg) or PBS. $n = 5$–6 mice/group. *$P < 0.05$, **$P < 0.01$ vs. PBS.

Considerable evidence attests to the importance of inflammation and innate immunity in the control of metabolism (35,36); however, few studies have examined whether IELs play a role in the development and/or treatment of experimental models of type 2 diabetes or obesity. Emerging data link cytokine and chemokine activity with control of enteroendocrine cell responses. Direct administration of RANTES (regulated on activation, normal T cell expressed and secreted) to NCIH716 cells rapidly reduces GLP-1 secretion and cAMP accumulation, and RANTES reduces plasma levels of GLP-1 and blunts the rise in insulin levels after glucose administration in vivo

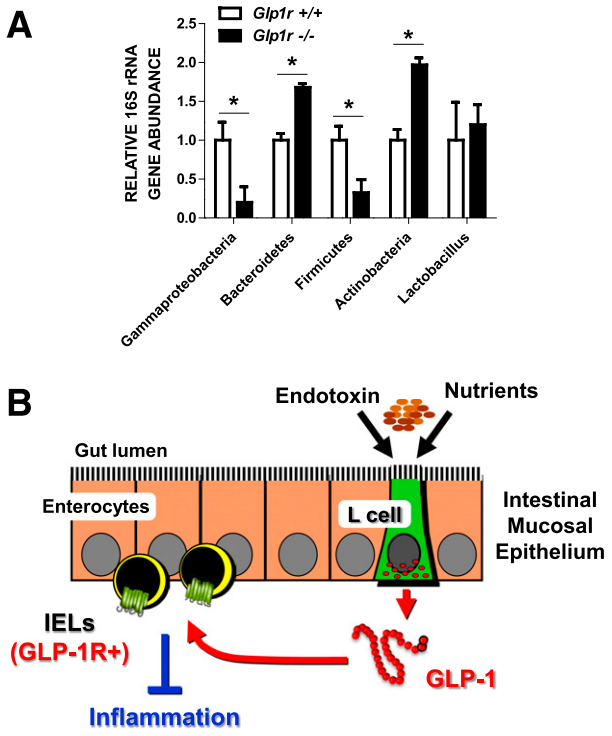

Figure 8—*A*: *Glp1r*$^{+/+}$ and *Glp1r*$^{-/-}$ mice exhibit significant differences in the relative abundance of several bacterial phyla. Comparisons were made using fecal samples from 11–14-week-old *Glp1r*$^{+/+}$ and *Glp1r*$^{-/-}$ female mice maintained on standard rodent chow and housed in groups of the same genotype per cage (n = 3–5 mice/group). *$P < 0.05$ for *Glp1r*$^{+/+}$ vs. *Glp1r*$^{-/-}$ mice. *B*: IELs and L cells define a local cellular network within the boundaries of the intestinal mucosal epithelium that translates information from the gut lumen (nutrients, bacterial products) through GLP-1 to control host mucosal immune responses through modulation of innate immunity.

(37). In contrast, IL-6, IL-1, and LPS all increase GLP-1 levels in mice (8–10), with IL-6 acting directly on gut endocrine cells to promote GLP-1 secretion. Of note, central blockade of GLP-1R signaling enhanced the pyrogenic effect of LPS (38), implying that endogenous GLP-1 exerts anti-inflammatory actions. Indeed, pharmacological administration of GLP-1R agonists has exerted anti-inflammatory actions in multiple studies through incompletely understood mechanisms (39). The current data extend previous observations by demonstrating that GLP-1 rapidly suppresses a proinflammatory cytokine program from activated intestinal IELs ex vivo, actions requiring a functional GLP-1R. Hence, induction of GLP-1 secretion following administration of cytokines or endotoxin has relevance beyond glucose control and leads to attenuation of the inflammatory response (Fig. 8*B*).

Previous studies examining the relationship between proglucagon-derived peptides and control of gut inflammation have focused on the related L-cell peptide GLP-2, which potently suppresses inflammation in experimental models of gut injury (40–42). Conversely, disruption of GLP-2R signaling was associated with increased bacterial colonization of the small bowel, reduced bactericidal activity, impaired Paneth cell responses (43), and enhanced susceptibility to gut injury and inflammation (43). The anti-inflammatory actions of GLP-2 are indirect, mediated through reduction of gut permeability (44,45). Indeed, modulation (both gain and loss) of GLP-2R signaling robustly modifies gut barrier function and the extent of inflammation in murine models of diabetes characterized by gut injury and endotoxemia (46). The current findings demonstrate that loss of GLP-1R signaling also enhances the susceptibility to gut injury, albeit through different mechanisms, involving the IEL-GLP-1R signaling system.

Germ-free mice exhibit increased levels of circulating GLP-1 and enhanced proglucagon expression in the murine brainstem (47) and distal gut (48), whereas microbial metabolites such as indole directly activate GLP-1 secretion from L cells (49). Collectively, these emerging findings link the gut microbiome and its metabolic byproducts with the control of central and peripheral GLP-1 production. Reduction of energy intake and malnutrition has been associated with defective immune responses, and accumulating evidence supports an intimate link among energy availability, nutrient sensing, and the regulation of the innate immune response (50). Of note, *Glp1r*$^{-/-}$ mice exhibit resistance to diet-induced obesity (51), increased relative abundance of *Bacteroidetes*, and reduced abundance of *Firmicutes* in their microbiota, whereas obese mice show a decrease in *Bacteroidetes* and an increase in *Firmicutes* (52). Collectively, the data establish a previously unrecognized local GLP-1-IEL-GLP-1R axis that may influence microbiome composition and the response to intestinal inflammation (Fig. 8*B*). Because considerable evidence supports a role for gut-derived inflammation in the pathophysiology of insulin resistance arising in subjects with obesity and diabetes (35), we hypothesize that GLP-1R agonists exert favorable nonglycemic actions in part through modulation of IEL-GLP-1R signaling. This hypothesis requires further validation through experimental models of metabolic dysfunction and inflammation.

Funding. P.M.S. holds operating grants for the Canadian Institutes of Health Research (MOP-89894 and IOP-92890) and is the recipient of a Canada Research Chair in Gastrointestinal Disease. D.J.D. was supported in part by a Canada Research Chair in Regulatory Peptides, a Banting & Best Diabetes Centre-Novo Nordisk Chair in Incretin Biology, and operating grant 123391 from the Canadian Institutes of Health Research.

Duality of Interest. D.J.D. received partial grant support from Novo Nordisk. D.J.D. has served as an advisor or consultant or speaker within the past 12 months for Arisaph Pharmaceuticals, Inc., Intarcia Therapeutics, Merck Research Laboratories, MedImmune, Novo Nordisk, NPS Pharmaceuticals, Inc., Receptos, Inc., and Sanofi. Mount Sinai Hospital receives partial operating grant support for other studies in the Drucker laboratory from GlaxoSmithKline, Merck, Novo Nordisk, and Sanofi. Neither D.J.D. nor his family members hold stock directly or indirectly in any of these companies. No other potential conflicts of interest relevant to this article were reported.

Author Contributions. B.Y., L.L.B., J.K., D.H., X.C., L.J.P., K.C.J.-H., W.Y., and K.W.A.B. contributed to the planning and carrying out of experiments, analysis of results, and writing and review of the manuscript. M.G.S., P.M.S., and D.J.D. contributed to the planning of experiments, analysis of results, and writing and review of the manuscript. D.J.D. is the guarantor of this work and, as such, had full access to all the data in the study and takes responsibility for the integrity of the data and the accuracy of the data analysis.

References

1. Drucker DJ. The role of gut hormones in glucose homeostasis. J Clin Invest 2007;117:24–32
2. Xiao Q, Boushey RP, Cino M, Drucker DJ, Brubaker PL. Circulating levels of glucagon-like peptide-2 in human subjects with inflammatory bowel disease. Am J Physiol Regul Integr Comp Physiol 2000;278:R1057–R1063
3. Eissele R, Göke R, Willemer S, et al. Glucagon-like peptide-1 cells in the gastrointestinal tract and pancreas of rat, pig and man. Eur J Clin Invest 1992;22: 283–291
4. Campbell JE, Drucker DJ. Pharmacology, physiology, and mechanisms of incretin hormone action. Cell Metab 2013;17:819–837
5. Drucker DJ, Nauck MA. The incretin system: glucagon-like peptide-1 receptor agonists and dipeptidyl peptidase-4 inhibitors in type 2 diabetes. Lancet 2006;368:1696–1705
6. Drucker DJ, Yusta B. Physiology and pharmacology of the enteroendocrine hormone glucagon-like peptide-2. Annu Rev Physiol 2014;76:561–583
7. Nauck MA. Is glucagon-like peptide 1 an incretin hormone? Diabetologia 1999;42:373–379
8. Ellingsgaard H, Hauselmann I, Schuler B, et al. Interleukin-6 enhances insulin secretion by increasing glucagon-like peptide-1 secretion from L cells and alpha cells. Nat Med 2011;17:1481–1489
9. Nguyen AT, Mandard S, Dray C, et al. Lipopolysaccharides-mediated increase in glucose-stimulated insulin secretion: involvement of the GLP-1 pathway. Diabetes 2014;63:471–482
10. Kahles F, Meyer C, Möllmann J, et al. GLP-1 secretion is increased by inflammatory stimuli in an IL-6-dependent manner, leading to hyperinsulinemia and blood glucose lowering. Diabetes 2014;63:3221–3229
11. Cheroutre H, Lambolez F, Mucida D. The light and dark sides of intestinal intraepithelial lymphocytes. Nat Rev Immunol 2011;11:445–456
12. Hansotia T, Baggio LL, Delmeire D, et al. Double incretin receptor knockout (DIRKO) mice reveal an essential role for the enteroinsular axis in transducing the glucoregulatory actions of DPP-IV inhibitors. Diabetes 2004;53:1326–1335
13. Lefrançois L, Lycke N. Isolation of mouse small intestinal intraepithelial lymphocytes, Peyer's patch, and lamina propria cells. Curr Protoc Immunol 2001; 4:3.19.1–3.19.16
14. Leung FW, Miller JC, Reedy TJ, Guth PH. Exogenous prostaglandin protects against acid-induced deep mucosal injury by stimulating alkaline secretion in rat duodenum. Dig Dis Sci 1989;34:1686–1691
15. Chen Y, Chou K, Fuchs E, Havran WL, Boismenu R. Protection of the intestinal mucosa by intraepithelial gamma delta T cells. Proc Natl Acad Sci U S A 2002;99:14338–14343
16. Panjwani N, Mulvihill EE, Longuet C, et al. GLP-1 receptor activation indirectly reduces hepatic lipid accumulation but does not attenuate development of atherosclerosis in diabetic male ApoE(-/-) mice. Endocrinology 2013;154:127–139
17. Auletta JJ, Devecchio JL, Ferrara JL, Heinzel FP. Distinct phases in recovery of reconstituted innate cellular-mediated immunity after murine syngeneic bone marrow transplantation. Biol Blood Marrow Transplant 2004;10:834–847
18. Chomczynski P, Sacchi N. Single-step method of RNA isolation by acid guanidinium thiocyanate-phenol-chloroform extraction. Anal Biochem 1987;162: 156–159
19. Hadjiyanni I, Siminovitch KA, Danska JS, Drucker DJ. Glucagon-like peptide-1 receptor signalling selectively regulates murine lymphocyte proliferation and maintenance of peripheral regulatory T cells. Diabetologia 2010;53:730–740
20. Assa A, Vong L, Pinnell LJ, et al. Vitamin D deficiency predisposes to adherent-invasive *Escherichia coli*-induced barrier dysfunction and experimental colonic injury. Inflamm Bowel Dis 2015;21:297–306
21. Huson DH, Mitra S, Ruscheweyh HJ, Weber N, Schuster SC. Integrative analysis of environmental sequences using MEGAN4. Genome Res 2011;21: 1552–1560
22. Pyke C, Knudsen LB. The glucagon-like peptide-1 receptor—or not? Endocrinology 2013;154:4–8
23. Richards P, Parker HE, Adriaenssens AE, et al. Identification and characterisation of glucagon-like peptide-1 receptor expressing cells using a new transgenic mouse model. Diabetes 2014;63:1224–1233
24. Bullock BP, Heller RS, Habener JF. Tissue distribution of messenger ribonucleic acid encoding the rat glucagon-like peptide-1 receptor. Endocrinology 1996;137:2968–2978
25. Qiu Y, Yang H. Effects of intraepithelial lymphocyte-derived cytokines on intestinal mucosal barrier function. J Interferon Cytokine Res 2013;33:551–562
26. Kronenberg M, Havran WL. Frontline T cells: gammadelta T cells and intraepithelial lymphocytes. Immunol Rev 2007;215:5–7
27. Campos RV, Lee YC, Drucker DJ. Divergent tissue-specific and developmental expression of receptors for glucagon and glucagon-like peptide-1 in the mouse. Endocrinology 1994;134:2156–2164
28. Kedees MH, Guz Y, Grigoryan M, Teitelman G. Functional activity of murine intestinal mucosal cells is regulated by the glucagon-like peptide-1 receptor. Peptides 2013;48:36–44
29. Schmidtler J, Dehne K, Allescher H-D, et al. Rat parietal cell receptors for GLP-1-(7-36) amide: northern blot, cross-linking, and radioligand binding. Am J Physiol 1994;267:G423–G432
30. Pyke C, Heller RS, Kirk RK, et al. GLP-1 receptor localization in monkey and human tissue: novel distribution revealed with extensively validated monoclonal antibody. Endocrinology 2014;155:1280–1290
31. Wang H, Steeds J, Motomura Y, et al. CD4+ T cell-mediated immunological control of enterochromaffin cell hyperplasia and 5-hydroxytryptamine production in enteric infection. Gut 2007;56:949–957
32. Selleri S, Palazzo M, Deola S, et al. Induction of pro-inflammatory programs in enteroendocrine cells by the Toll-like receptor agonists flagellin and bacterial LPS. Int Immunol 2008;20:961–970
33. Qian BF, Hammarström ML, Danielsson A. Differential expression of vasoactive intestinal polypeptide receptor 1 and 2 mRNA in murine intestinal T lymphocyte subtypes. J Neuroendocrinol 2001;13:818–825
34. Bogunovic M, Davé SH, Tilstra JS, et al. Enteroendocrine cells express functional Toll-like receptors. Am J Physiol Gastrointest Liver Physiol 2007;292: G1770–G1783
35. Jin C, Henao-Mejia J, Flavell RA. Innate immune receptors: key regulators of metabolic disease progression. Cell Metab 2013;17:873–882
36. Hotamisligil GS. Inflammation and metabolic disorders. Nature 2006;444: 860–867
37. Pais R, Zietek T, Hauner H, Daniel H, Skurk T. RANTES (CCL5) reduces glucose-dependent secretion of glucagon-like peptides 1 and 2 and impairs glucose-induced insulin secretion in mice. Am J Physiol Gastrointest Liver Physiol 2014;307:G330–G337
38. Rinaman L, Comer J. Antagonism of central glucagon-like peptide-1 receptors enhances lipopolysaccharide-induced fever. Auton Neurosci 2000;85: 98–101
39. Drucker DJ, Rosen CF. Glucagon-like peptide-1 (GLP-1) receptor agonists, obesity and psoriasis: diabetes meets dermatology. Diabetologia 2011;54:2741–2744
40. Boushey RP, Yusta B, Drucker DJ. Glucagon-like peptide (GLP)-2 reduces chemotherapy-associated mortality and enhances cell survival in cells expressing a transfected GLP-2 receptor. Cancer Res 2001;61:687–693
41. Drucker DJ, Yusta B, Boushey RP, DeForest L, Brubaker PL. Human [Gly2]GLP-2 reduces the severity of colonic injury in a murine model of experimental colitis. Am J Physiol 1999;276:G79–G91

42. Boushey RP, Yusta B, Drucker DJ. Glucagon-like peptide 2 decreases mortality and reduces the severity of indomethacin-induced murine enteritis. Am J Physiol 1999;277:E937–E947
43. Lee S-J, Lee J, Li KK, et al. Disruption of the murine Glp2r impairs Paneth cell function and increases susceptibility to small bowel enteritis. Endocrinology 2012;153:1141–1151
44. Hadjiyanni I, Li KK, Drucker DJ. Glucagon-like peptide-2 reduces intestinal permeability but does not modify the onset of type 1 diabetes in the nonobese diabetic mouse. Endocrinology 2009;150:592–599
45. Bahrami J, Longuet C, Baggio LL, Li K, Drucker DJ. Glucagon-like peptide-2 receptor modulates islet adaptation to metabolic stress in the ob/ob mouse. Gastroenterology 2010;139:857–868
46. Cani PD, Possemiers S, Van de Wiele T, et al. Changes in gut microbiota control inflammation in obese mice through a mechanism involving GLP-2-driven improvement of gut permeability. Gut 2009;58:1091–1103
47. Schéle E, Grahnemo L, Anesten F, Hallén A, Bäckhed F, Jansson JO. The gut microbiota reduces leptin sensitivity and the expression of the obesity-suppressing neuropeptides proglucagon (Gcg) and brain-derived neurotrophic factor (Bdnf) in the central nervous system. Endocrinology 2013;154:3643–3651
48. Wichmann A, Allahyar A, Greiner TU, et al. Microbial modulation of energy availability in the colon regulates intestinal transit. Cell Host Microbe 2013;14: 582–590
49. Chimerel C, Emery E, Summers DK, Keyser U, Gribble FM, Reimann F. Bacterial metabolite indole modulates incretin secretion from intestinal enteroendocrine L cells. Cell Reports 2014;9:1202–1208
50. Tsalikis J, Croitoru DO, Philpott DJ, Girardin SE. Nutrient sensing and metabolic stress pathways in innate immunity. Cell Microbiol 2013;15:1632–1641
51. Hansotia T, Maida A, Flock G, et al. Extrapancreatic incretin receptors modulate glucose homeostasis, body weight, and energy expenditure. J Clin Invest 2007;117:143–152
52. Hartstra AV, Bouter KE, Bäckhed F, Nieuwdorp M. Insights into the role of the microbiome in obesity and type 2 diabetes. Diabetes Care 2015;38: 159–165

SUPPLEMENTARY DATA

Cellular Fractionation of Mouse Small Intestine

Cellular fractionation of the mouse small intestine was performed as described (13). Briefly, the small intestine was removed, flushed with saline, opened and cut into 5-10 mm segments. The tissue was rinsed in calcium and magnesium-free Hank's balanced salt solution (HBSS-/-) containing 10 mM EDTA and then subjected to sequential digestion with collagenase XI (1 mg/ml HBSS-/-, Sigma-Aldrich Canada, Oakville, ON). Cells released after each digestion (referred to as 'fraction 1' and 'fraction 2') were recovered by centrifugation and used for quantitative RNA analysis.

Flow Cytometry

Freshly isolated Percoll-purified IELs were treated with Fc block (anti-mouse CD16/CD32 mAb, BD Biosciences Canada, Mississauga, ON) for 15 min at 4°C. Cell surface staining was then performed by incubation for 30 min at 4°C with fluorochrome-coupled anti-mouse CD45, CD3ε, CD19, CD4, CD8α, CD8β, TCRβ and TCRγδ mAbs obtained from BD Biosciences or eBioscience (San Diego, CA). A viability marker (DAPI or 7-AAD) was included to discriminate live cells. Stained cells were analyzed on a Gallios flow cytometer (Beckman Coulter Canada, Mississauga, ON). Data analysis was performed using Kaluza software (Beckman Coulter Canada). For FACS enrichment, pooled Percoll-purified IELs from 2-6 mice were labeled with the appropriate antibodies and sorted on a MoFlo Astrios instrument (Beckman Coulter Canada). Live untouched intestinal IELs were also obtained from pooled Percoll-purified IELs by sorting using forward and side scatter features in combination with viability staining. Post-sorting purity was consistently >96% and viability >97%.

Determination of Cytokine/Chemokine Levels

Protein levels of IFNγ, IL-1β, Il-2, Il-6, Il-13, TNFα and Cxcl1 were quantified in jejuna extracts, and media from cultured IELs using a Cytometric Bead Array assay kit (BD Biosciences). Jejunal extracts were homogenized in PBS containing 0.5% Triton X-100 and protease inhibitor cocktail (Sigma-Aldrich Canada). Homogenates were centrifuged at 16,000g for 20 min at 4°C, supernatants collected, and total protein content determined using a bicinchoninic acid (BCA) assay kit (Pierce, Rockford, IL).

SUPPLEMENTARY DATA

Supplementary Figure 1. (A) *Glp1r* expression segregates with markers of the villus epithelial compartment following cellular fractionation of the mouse small intestine. Fractions 1 and 2 correspond to cell fractions obtained following sequential collagenase XI digestion of the small intestine. Transcript levels for the different cell lineage markers are expressed relative to the corresponding jejunal mRNA levels and are mean±SD of 5 independent fractionation experiments. *iFabp*, intestinal fatty acid binding protein; *Clca3*, chloride channel calcium activated 3; *ChrA*, chromogranin A; *Crypt5*, cryptdin 5; *Uchl1*, ubiquitin carboxy-terminal hydrolase L1. (B) *Glp1r* expression along the mouse intestine correlates with the abundance of IEL markers. mRNA levels in duodenum (Duo), proximal (P), mid (M) and distal (D) jejunum (Jej), ileum (Ile) and colon are expressed relative to the corresponding transcript levels in the duodenum and are mean±SD (n=4 mice). (C) Contrasting sensitivity to forskolin among different murine lymphoid cell populations. Levels of cAMP were quantified in sorted untouched IELs, splenocytes, and thymocytes following incubation with either veh, Ex-4 or Fk. Data are expressed relative to the corresponding cAMP levels in veh-treated cells and are mean ±SD from two independent experiments with 2-3 replicates each (IELs) or from a single experiment performed in triplicate (splenocytes and thymocytes). (D) Exendin(9-39) antagonizes exendin-4 suppression of cytokine induction in activated IELs. Sorted untouched IELs were activated with anti-CD3/CD28 for 5 h in the presence of Ex-4 (3 nM) or vehicle (Veh) with or without exendin(9-39) (1 μM). mRNA levels of the indicated cytokines were assessed by qPCR. Data are mean±SD of a single experiment assayed in triplicate. (E) Exendin-4 suppresses cytokine protein levels in activated IELs from *Glp1r*$^{+/+}$ mice. Sorted untouched IELs were activated with anti- CD3/CD28 for 5 h (IFNγ, top panel) or 16 h (TNFα, bottom panel) in the presence of Ex-4 or vehicle (Veh). Levels of the indicated cytokines were assessed by cytometric bead assay. Data are mean±SD and representative of one out of three independent experiments. Values for the non-activated Veh-treated IELs were below the detection limit of the assay. ***= P, .001.

SUPPLEMENTARY DATA

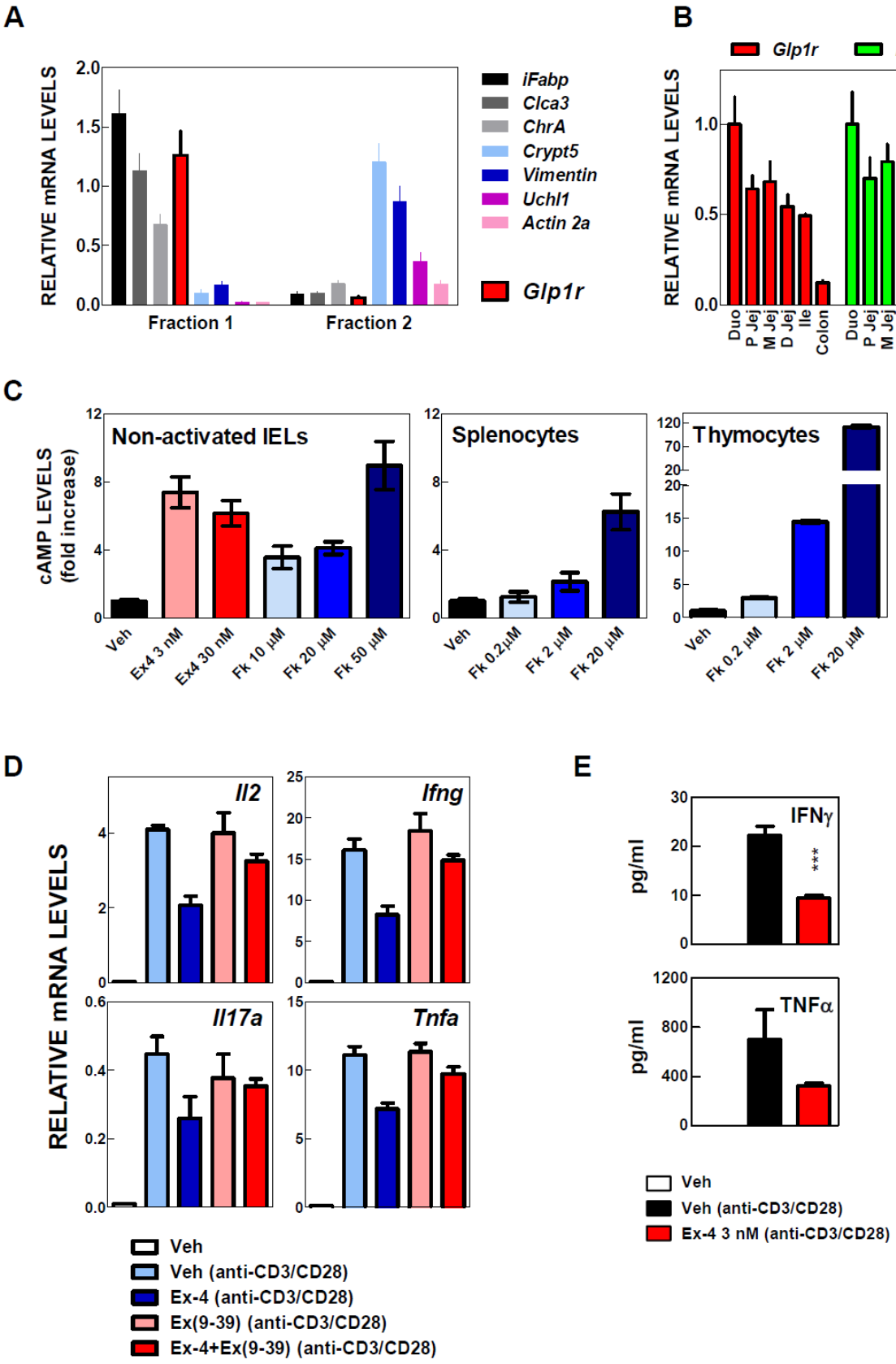

SUPPLEMENTARY DATA

Supplementary Figure 2. Gene expression in colon samples of *Glp1r*$^{+/+}$ vs *Glp1r*$^{-/-}$ mice following 7 days of exposure to drinking water containing 3% DSS or regular drinking water (veh). n=9-12 mice/group. *, **, *** $p<0.05$, $p<0.01$ and $p<0.001$, respectively, for *Glp1r*$^{+/+}$ vs *Glp1r*$^{-/-}$ on DSS drinking water.

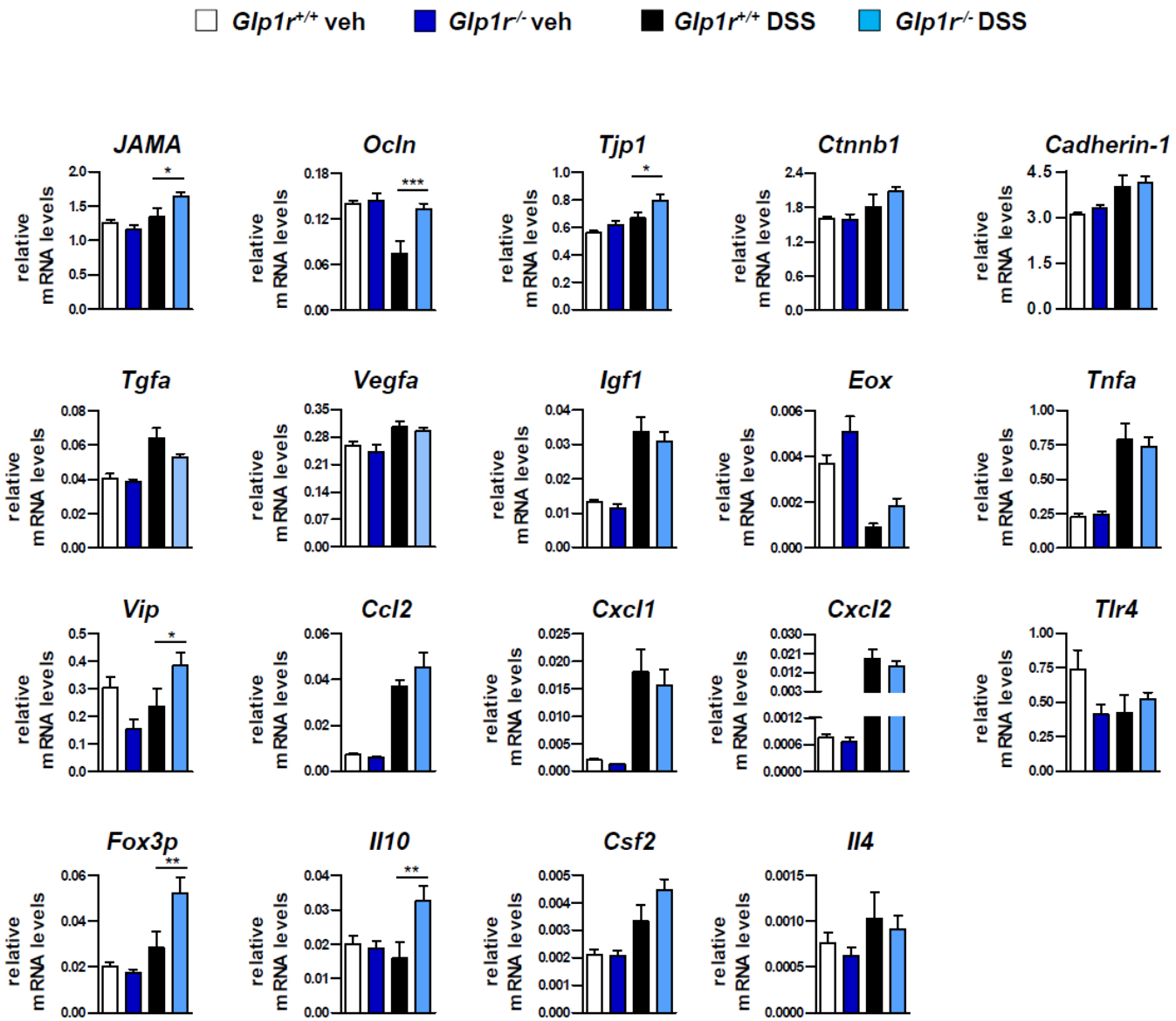

SUPPLEMENTARY DATA

Supplementary Figure 3. (A) Small bowel permeability of 3-month-old *Glp1r*$^{+/+}$ and *Glp1r*$^{-/-}$ male mice. Mice were fasted overnight (16 h) and then given an oral gavage of 200 μl of PBS containing 0.4 μCi D-[1-14C]-mannitol (Perkin Elmer, Waltham, MA). Blood samples (50 μl) were collected from the tail vein after 0, 30, 60, 120 and 180 min and the amount of radioactivity in plasma determined by scintillation counting. (B) Quantitative assessment of *Glp1r* expression in jejunum (left panel) and sorted small intestinal IELs (right panel) from recipient *Glp1r*$^{-/-}$ female mice reconstituted with bone marrow from C57BL/6 donor male mice. The TaqMan expression assay targeting exons 3-4 of the murine *Glp1r* mRNA detects both wild-type and knockout *Glp1r* transcripts, whereas the assay targeting exons 5-6 only detects the wild-type *Glp1r* mRNA. *Glp1r* transcript levels are expressed relative to the *Glp1r* mRNA levels in *Glp1r*$^{+/+}$ recipient mice (grey horizontal stripe). Shown are combined data from 2 independent bone marrow transfer experiments. Each data point corresponds to one mouse. (C) Cytokine protein levels in jejunal extract samples from C57BL/6 mice that were given a single i.p. injection of Ex-4 (10 nmol/kg) or PBS and then sacrificed 4 h later. n=5 samples per treatment. **, ***$p<0.01$ and $p<0.001$, respectively for Ex-4- vs PBS-treated mice. IL-6 and TNFα protein levels for PBS-treated mice were below the detection limit of the assay and assigned a value of 0. (D) Colon damage score in C57BL/6 mice maintained on drinking water supplemented with 3% DSS for 4 days followed by 2 injections (12 h apart) of Ex-4 (10 nmol/kg) or PBS. n=6 mice/group.

SUPPLEMENTARY DATA

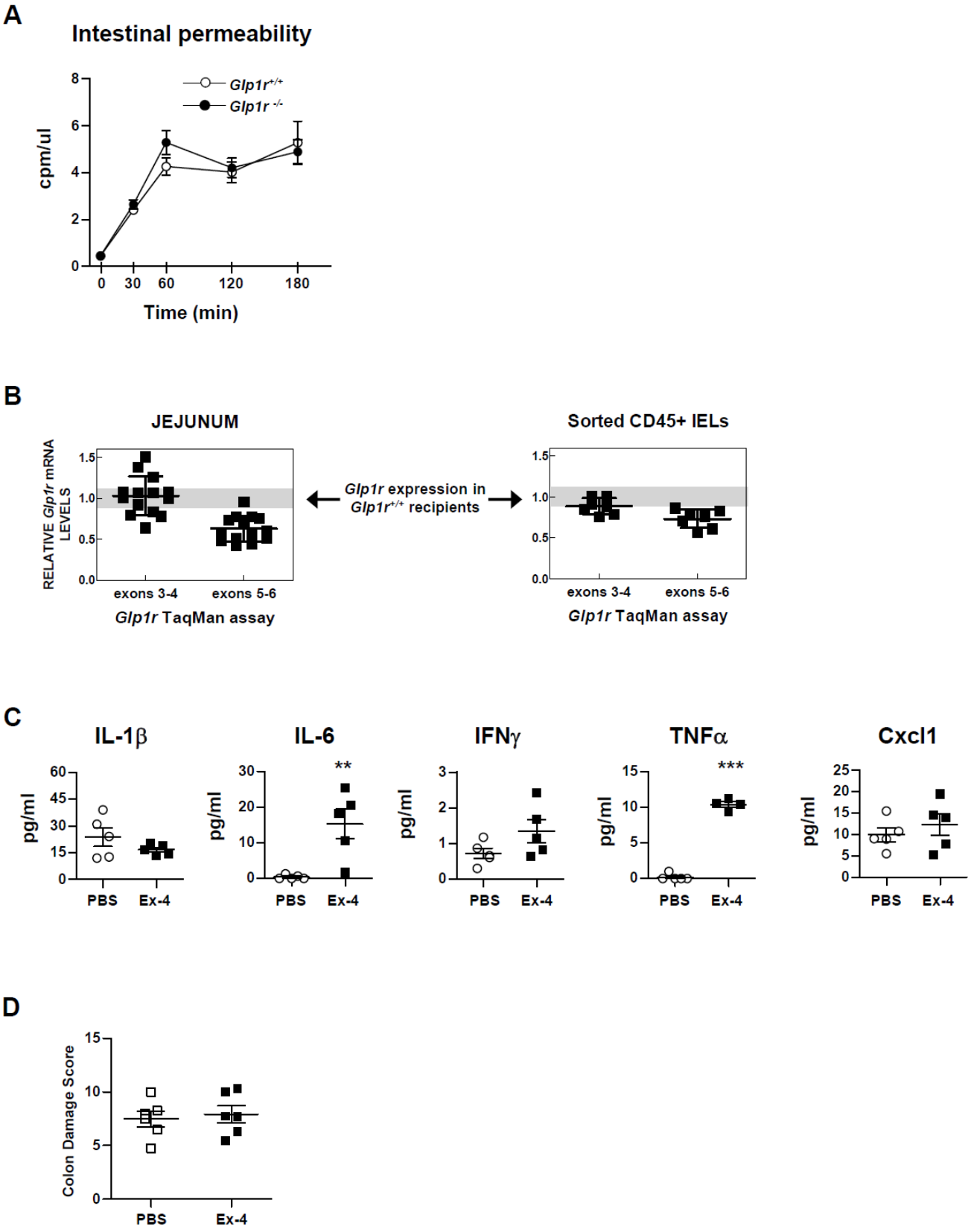

SUPPLEMENTARY DATA

Supplementary Figure 4. (A-B) Relative abundance of microbial communities in fecal samples from *Glp1r*$^{+/+}$ and *Glp1r*$^{-/-}$ mice. *Bacteroidetes* (light brown) and *Firmicutes* (yellow) represent the major bacterial populations in *Glp1r*$^{+/+}$ and *Glp1r*$^{-/-}$ mice. Each bar indicates the microbial composition of one mouse. MEtaGenome Analysis (MEGAN) was performed to determine microbial population similarities within and between groups of *Glp1r*$^{+/+}$ and *Glp1r*$^{-/-}$ mice. The cluster analysis tree was generated using UPGMA cluster analysis of Bray-Curtis dissimilarity coefficients.

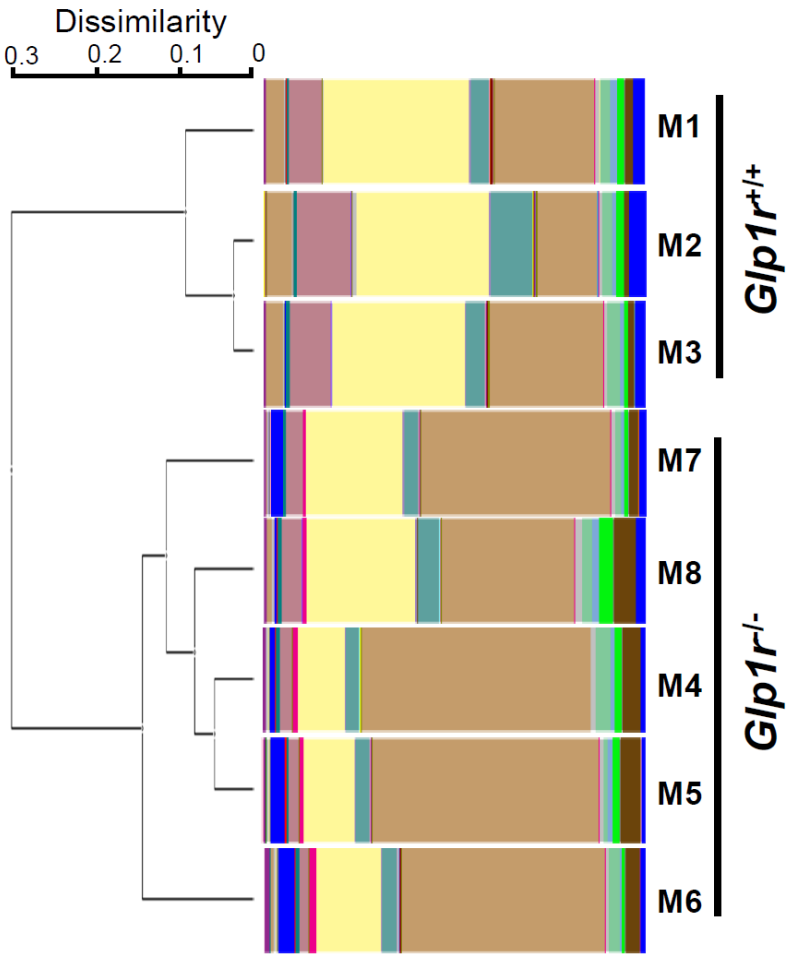

SUPPLEMENTARY DATA